

Recovery of eigenvectors from eigenvalues in systems of coupled harmonic oscillators

Henning U. Voss* & Douglas J. Ballon

Citigroup Biomedical Imaging Center and Department of Radiology, Weill Cornell Medicine, New York, NY, USA

*Corresponding author. Email: hev2006@med.cornell.edu

Abstract —The eigenvector-eigenvalue identity relates the eigenvectors of a Hermitian matrix to its eigenvalues and the eigenvalues of its principal submatrices in which the j th row and column have been removed. We show that one-dimensional arrays of coupled resonators, described by square matrices with real eigenvalues, provide simple physical systems where this formula can be applied in practice. The subsystems consist of arrays with the j th resonator removed, and thus can be realized physically. From their spectra alone, the oscillation modes of the full system can be obtained. The principle of successive single resonator deletions is demonstrated in two experiments of coupled radiofrequency resonators, in which the spectra are measured with a network analyzer. Both the Hermitian as well as a non-Hermitian case are covered in the experiment. In both cases the experimental eigenvector estimates agree well with numerical simulations if certain consistency conditions imposed by system symmetries are taken into account. In the Hermitian case, these estimates are obtained only from resonance spectra without knowledge of the system parameters. It remains an interesting problem of physical relevance if the full non-Hermitian eigenvector set can be obtained from the spectrum alone.

Key words—harmonic oscillator arrays, radiofrequency resonators, spectroscopy, magnetic resonance imaging, linear algebra

I. INTRODUCTION

The eigenvector-eigenvalue identity [1, 2] relates the eigenvectors of Hermitian matrices to their eigenvalues and the eigenvalues of the principal submatrices obtained by removing the j th row and column. It has been applied recently to a problem in theoretical physics where it was difficult to compute eigenvectors directly [3], and in graph theory to assess robustness of networks with respect to removal of network nodes [4]. The identity has recently been generating considerable interest in its origin and applications [2]. In general, it may be particularly useful in the study of physical systems where only the spectrum (eigenvalues) of a system described by a Hermitian matrix can be measured, but the modes (eigenvectors) are inaccessible. This situation is often encountered in spectroscopy [5]. Here it is demonstrated that the identity applies to coupled oscillator systems in a way that suggests a simple experimental procedure for recovery of the eigenvectors. The oscillation modes are conventionally obtained as a solution of the eigenvalue problem of the system interaction matrix. If the system matrix is unknown, one can use the eigenvector-eigenvalue identity to obtain the modes from measurements of the system's spectrum and its subspectra by successively removing and replacing each oscillator. This “successive single deletion procedure” will be applied to one-dimensional arrays of coupled radiofrequency (RF) resonators, a system that is easily realized in the laboratory.

The organization of this Letter is as follows: First, it is shown that coupled oscillator systems are amenable to analysis by the eigenvector-eigenvalue identity. The successive single deletion procedure is then applied to a coupled oscillator model, which is used to estimate the eigenvectors in one-dimensional array experiments. A brief discussion concludes this Letter.

II. OSCILLATOR SYSTEMS

The eigenvector-eigenvalue identity relates the j th component of the i th eigenvector v of a Hermitian $N \times N$ matrix H to its real eigenvalues $\lambda_n(H)$ ($n = 1 \dots N$) and the real eigenvalues $\lambda_n(H_j)$ ($n = 1 \dots N-1$) of the principal submatrices H_j obtained by removing the j th row and column from H . Stated in a form that avoids case distinctions for the occurrence of zero terms, it reads

$$|v_{i,j}|^2 \prod_{k=1; k \neq i}^N [\lambda_i(H) - \lambda_k(H)] = \prod_{k=1}^{N-1} [\lambda_i(H) - \lambda_k(H_j)]. \quad (1)$$

This identity can be used to obtain the eigenvector components $|v_{i,j}|$ directly from the eigenvalues of matrix H and the principal submatrices H_j . These modes are called ‘‘Thompson modes’’ in the following.

In coupled oscillator arrays, the principal submatrices can be obtained by succesively removing and replacing each oscillator in the array. This will be shown in the example of coupled RF oscillators but can be extended to other physical systems, for example mechanical oscillators [6]. Arrays of N inductively coupled LC resonators with identical geometries, i.e., identical inductances $L_n = L$, are considered here. The mutual inductances between array elements n and $n+1$ are $M_n = \kappa_n L$, where κ_n denotes the coupling coefficient between array elements n and $n+1$, and there are $N-1$ couplings. The κ_n are dimensionless real numbers and depend on the distances between resonators. The capacitances C_n can be individually set to different values. It is further assumed that the electromagnetic wavelength is large compared to the linear dimensions of the network, such that the near-field regime holds. With the assumption of only nearest-neighbor coupling and the impedance of each isolated element given by $i\omega L + \frac{1}{i\omega C_n}$, the Kirchhoff equations for the currents I_n in the array read

$$\frac{1}{LC_n} I_n = \omega^2 (I_n + \kappa_{n-1} I_{n-1} + \kappa_n I_{n+1}), \quad (2)$$

with $n = 1 \dots N$ and fixed-edge boundary conditions $I_0 = I_{N+1} = \kappa_0 = \kappa_N = 0$. For the more general case of non-local couplings, which are studied here, it is advantageous to rewrite the Kirchhoff equations in matrix notation [7, 8] as

$$HI = \lambda I \text{ with } H = CM \text{ and } \lambda = \omega^{-2}. \quad (3)$$

The N oscillator modes each consist of the N current amplitudes I_n , and the spectrum consists of the inverse squared resonance frequencies. The capacitance matrix C is diagonal with $C_{nn} = C_n$, and the matrix M contains the magnetic components L and κ_k of the system. Its diagonal elements are L . Depending on the number of array elements involved in the coupling to element n , M has multiple non-zero off-diagonal elements. For example, for nearest neighbor coupling and identical spacing between neighbors, the off-diagonal elements would be $\kappa_L L$, with a constant coupling coefficient κ_L . The matrix M for greater-than-nearest-neighbor coupling is given here for the case of $N = 5$ coupled oscillators, which will be used in the experiment below. It is

$$M = L \begin{pmatrix} 1 & \kappa_1 & \kappa_2 & \kappa_3 & \kappa_4 \\ \kappa_1 & 1 & \kappa_1 & \kappa_2 & \kappa_3 \\ \kappa_2 & \kappa_1 & 1 & \kappa_1 & \kappa_2 \\ \kappa_3 & \kappa_2 & \kappa_1 & 1 & \kappa_1 \\ \kappa_4 & \kappa_3 & \kappa_2 & \kappa_1 & 1 \end{pmatrix}. \quad (4)$$

This coupling scheme was chosen since it best approximated the measured couplings of the experimental system as described below. The system matrix is

$$H = CM = L \begin{pmatrix} C_1 & \kappa_1 C_1 & \kappa_2 C_1 & \kappa_3 C_1 & \kappa_4 C_1 \\ \kappa_1 C_2 & C_2 & \kappa_1 C_2 & \kappa_2 C_2 & \kappa_3 C_2 \\ \kappa_2 C_3 & \kappa_1 C_3 & C_3 & \kappa_1 C_3 & \kappa_2 C_3 \\ \kappa_3 C_4 & \kappa_2 C_4 & \kappa_1 C_4 & C_4 & \kappa_1 C_4 \\ \kappa_4 C_5 & \kappa_3 C_5 & \kappa_2 C_5 & \kappa_1 C_5 & C_5 \end{pmatrix}. \quad (5)$$

One observes that unlike M this matrix is not symmetric and thus no longer Hermitian in general. However, Since C is diagonal and positive definite, and M is symmetric, the product CM has real eigenvalues. There are two cases to be distinguished, and our two examples to follow match these cases:

1. All capacitances are equal. Then C is a constant diagonal matrix and H is Hermitian. In this case, the eigenvector-eigenvalue identity can be applied without further adjustments.

2. Not all capacitances are equal and H is not Hermitian. For this case we first note that $H = CM$ has the same spectrum as the Hermitian matrix $C^{\frac{1}{2}} M C^{\frac{1}{2}}$. This follows from

$$\det(\lambda I - CM) = \det \left[C^{\frac{1}{2}} \left(\lambda I - C^{\frac{1}{2}} M C^{\frac{1}{2}} \right) C^{-\frac{1}{2}} \right] = \det C^{\frac{1}{2}} \det \left(\lambda I - C^{\frac{1}{2}} M C^{\frac{1}{2}} \right) \det C^{-\frac{1}{2}} = 0. \quad (6)$$

In other words, the matrix $C^{\frac{1}{2}} M C^{\frac{1}{2}}$ is symmetric with real eigenvalues, and the eigenvalues of CM and of $C^{\frac{1}{2}} M C^{\frac{1}{2}}$ are identical. There are now two systems with identical spectra, CM and $C^{\frac{1}{2}} M C^{\frac{1}{2}}$, but with in general different eigenvectors. Since the eigenvector-eigenvalue identity is designed to only find the Hermitian system, an additional step is required to obtain the correct eigenvector estimates for the non-Hermitian case. Denoting the eigenvector matrix of the Hermitian case with T and the matrix of eigenvalues with Λ , its eigendecomposition reads

$$T^{-1} C^{\frac{1}{2}} M C^{\frac{1}{2}} T = \Lambda. \quad (7)$$

Note that T is also the matrix obtained from an application of the eigenvector-eigenvalue identity to the non-Hermitian system $H = CM$, because it has the same spectrum. The equivalent eigendecomposition for the non-Hermitian case reads

$$U^{-1} C M U = \Lambda. \quad (8)$$

From these two equations follows that the correct eigenvector matrix U for the system $H = CM$ can be obtained from the transformation

$$U = C^{\frac{1}{2}} T. \quad (9)$$

In summary, in order to obtain the correct eigenvector estimates from a system described by the generally non-Hermitian matrix $H = CM$, first the eigenvectors of the similar Hermitian matrix $C^{\frac{1}{2}}MC^{\frac{1}{2}}$ are obtained with the eigenvector-eigenvalue identity, and then Eq. (9) is used to transform those into the eigenvectors of H . The price to pay for non-Hermiticity is that the capacitances of the system, or at least their ratios, have to be known a-priori.

Remark: The matrices CM and $C^{\frac{1}{2}}MC^{\frac{1}{2}}$ are just two elements of a continuum of matrices that have all the same spectrum and are defined by $C^\alpha MC^{1-\alpha}$ ($\alpha \in [0,1]$). The matrix CM arises from $\alpha = 1$ and $C^{\frac{1}{2}}MC^{\frac{1}{2}}$ from $\alpha = \frac{1}{2}$. However, their eigenvectors differ in general, and the eigenvector-eigenvalue identity only recovers the symmetric case with $\alpha = \frac{1}{2}$.

III. THE SUCCESSIVE SINGLE DELETION PROCEDURE IN THE MODEL

The procedure to obtain eigenvectors from eigenvalues via the eigenvector-eigenvalue identity has the following correspondence in this model: Removing the j th LC resonator amounts to removing the j th row and column of both the capacitance matrix C and the magnetic matrix M . Fortunately, as C is diagonal, the procedure has the same effect on the product matrix $H = CM$. This is the key requirement to be able to apply the eigenvector-eigenvalue identity to this system. Specifically, taking out the second oscillator, for example, the corresponding principal submatrix would be

$$H_2 = L \begin{pmatrix} C_1 & \kappa_2 C_1 & \kappa_3 C_1 & \kappa_4 C_1 \\ \kappa_2 C_3 & C_3 & \kappa_1 C_3 & \kappa_2 C_3 \\ \kappa_3 C_4 & \kappa_1 C_4 & C_4 & \kappa_1 C_4 \\ \kappa_4 C_5 & \kappa_2 C_5 & \kappa_1 C_5 & C_5 \end{pmatrix}. \quad (10)$$

One can see that now the first oscillator couples to the third one (via coupling κ_2), without involving the second oscillator (coupling κ_1). Since the distances and thus the couplings themselves do not change, the correct coupling between the first and the third oscillator is indeed given by κ_2 .

Numerical solutions of Eq. (1) for two different arrays with $N = 5$ oscillators were obtained with Matlab (The Mathworks, version R2017a). The code is provided in the Appendix. It also contains specific model parameters such as L , C_1 , C_2 , and the coupling coefficients κ_1 to κ_4 . The two arrays are defined as follows:

1. (Hermitian case) An array with identical capacitances $C_1 = C_2 = \dots = C_5$, which are all defined to correspond to an LC resonator angular base frequency of $\omega = (LC_1)^{-1/2}$, or $f = 200$ MHz.
2. (Non-Hermitian case) A dimeric array with alternating capacitances, $C_1 = C_3 = C_5$, corresponding to a frequency of $f = 200$ MHz, and $C_2 = C_4$ corresponding to $f = 220$ MHz. Such a dimeric array exhibits a band gap that is evident with five elements but evolves more fully in the asymptotic limit of infinite N [9].

The results are provided in Fig. 1. The spectra of system 1 and 2 are shown in the left panels of Fig. 1A and B, respectively. The bold black lines denote the location of the five principal eigenvalues of H . The thin gray lines denote the location of the 5×4 eigenvalues of the five principal submatrices H_j . Due to symmetry, removal of the fourth and fifth resonator duplicates the eigenvalues from the removal of the first and second resonator, and therefore, only 3×4 distinct subsystem eigenvalues are visible in the spectrum. In the right panels the model modes $|v_{i,j}|$ are displayed in black and, overlaid to them in gray, the Thompson modes

obtained via Eq. (1). For the non-Hermitian dimeric system, the additional step of the similarity transform, Eq. (9), has been applied. In both cases, the model modes and Thompson modes are identical.

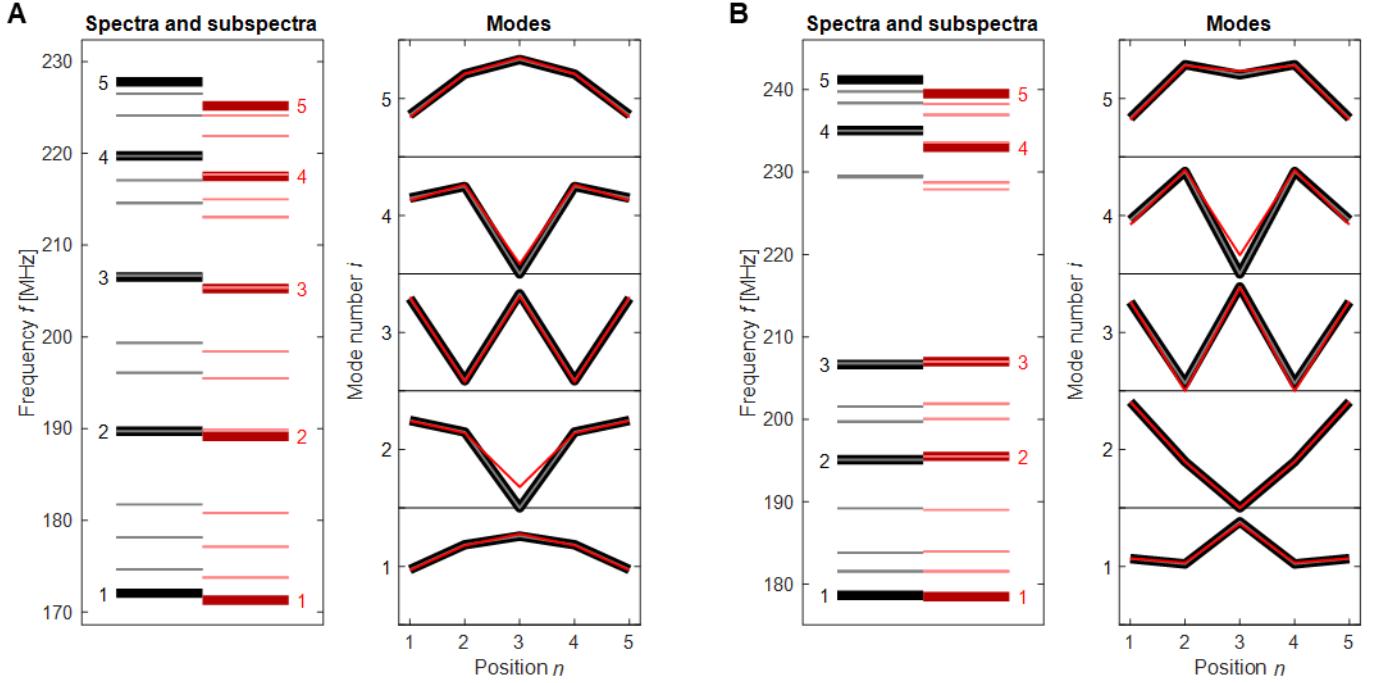


Figure 1 (color): Obtaining eigenvectors of radiofrequency resonator arrays via the eigenvalue-eigenvector identity. A) Left image: Model spectrum (black) and subspectra (gray), and measured spectrum (dark red) and subspectra (light red) for a system of five coupled identical RF resonators. Right image: Model eigenvectors (black), model-based Thompson modes (gray), and experimental Thompson modes estimated from the measured spectra shown in the left image (red). B) The same graphs as shown in A) but for a dimeric system with a band gap as explained in the text.

IV. THE SUCCESSIVE SINGLE DELETION PROCEDURE IN THE EXPERIMENT

The resonator arrays were comprised of $N = 5$ rectangular LC loops that were aligned coaxially and have been described in detail previously [9]. Individual resonators were tuned by a trim capacitor to their base frequencies, which are defined as the resonance frequencies of the isolated, uncoupled, elements. The base frequencies match those used in the numerical simulations of the systems. Thus, the two systems are 1. A system with identical base frequencies of 200 MHz in each of the resonators, and 2. A dimeric system with two alternating base frequencies of 200 and 220 MHz. The spectra of these systems were measured by a network analyzer (Agilent 85046A) with an S-parameter test set. The arrays were inductively coupled to the network analyzer by a loop similar to the LC resonators, without the capacitor. Specifically, the absolute value of the S_{11} input port voltage reflection coefficient versus frequency provided the spectra and subspectra. Spectral peak frequencies were identified by an automatic peak search algorithm. They are provided in the Matlab script.

In order to obtain the Thompson modes from spectra that have unavoidable measurement errors, some adjustments need to be applied to ensure consistency between the measured principal spectrum and the subspectra. Note that the ordered spectrum and subspectra of symmetric matrices A are tightly linked to each other via the Cauchy interlacing inequalities for diagonalizable matrices [2]. These state that the i th eigenvalue of each principal submatrix A_j is confined to the interval spanned by the i th and $i+1$ st eigenvalue

of A . The Cauchy interlacing inequalities are a necessary condition for A being Hermitian. It has already been shown in Eq. (6) that the characteristic polynomials of the nearly-symmetric matrices $H = CM$, Eq. (3), can be written as characteristic polynomials of real symmetric matrices, such that these inequalities remain valid. However, measurement errors can cause a violation of the Cauchy interlacing inequalities. Measurements also cannot resolve degenerate spectral resonances or resonances that are too close to each other. In the following, a workflow to handle these complications is provided.

The successive single deletion procedure to obtain modes from experimental spectra

1. Measure the spectrum of the system and estimate the spectral peak locations.
2. Remove the first resonator and measure the resulting subspectrum.
3. Replace the first resonator, remove the second one, and proceed until all N subspectra have been measured.
4. Sort the spectra in ascending order.
5. Symmetrize the subspectra according to the symmetry inherent in the array. For example, for the described five-element arrays, removing the first or the fifth, or similarly, the second or the fourth elements should each provide the same subspectra, but the measurements generally differ. In this case, symmetrization is performed by averaging the first and fifth, and the second and fourth measurements. It turns out that although the measured spectra are already approximately symmetric, this step improves the symmetry of the estimated Thompson modes noticeably.
6. Reconcile the measurements with the Cauchy interlacing inequalities. Measured eigenvalues not adhering to these inequalities are a-posteriori minimally modified to fit into the scheme. For example, if a value is larger than the upper bound specified by the corresponding Cauchy interlacing inequality, it is set to the upper bound. This step helps prevent negative squared mode components. The commentaries in the supplemental Matlab script detail this step for the two experiments. It turns out that the necessary adjustments are relatively small.
7. Estimate the Thompson modes from the modified measurements via Eq. (1). In order to identify zero mode components, $|v_{i,j}| = 0$, a numerical threshold is defined that assigns a zero to very small values of the right hand side of Eq. (1). It has been observed that this step contributes to the stability of the procedure including avoiding small negative squared components.
8. For non-Hermitian systems, correct the Thompson modes with Eq. (9).
9. Normalize the estimated Thompson modes in order to compensate for estimation errors.

The spectra of system 1 and 2 are shown in the left panels of Fig. 1A and B, respectively. The bold red lines denote the location of the measured spectral peaks of the resonator array and the thin bright red lines the spectral peak locations of the arrays in which one element has been removed. The right panels contain the experimental Thompson modes in red, overlaid to the black true eigenvectors and gray model Thompson modes. The experimental Thompson modes match the model Thompson modes. Small deviations can occur for at least two reasons. First, the real system modes are not known but are modeled based on Eq. (3). They depend on the validity of the model equations and accuracy of system parameter estimates that also have an error. Second, errors in the measurements of the eigenvalues propagate into the computation of the eigenvectors via Eq. (1).

V. DISCUSSION

It has been demonstrated that the eigenvector-eigenvalue identity is a useful tool to estimate the modes of Hermitian coupled oscillator systems even when the system parameters are not known and the modes cannot be measured directly. This simple formula states that the eigenvalues of a system and specific subsystems encode most of the information about the system dynamics, except phase information. This is remarkable in that explicit knowledge of the system equations besides their symmetry properties is not

required. For a special non-Hermitian case, an equivalent solution has been described that involves the a-priori inclusion of some system parameters.

The mathematical procedure of obtaining the necessary principal submatrices of the system matrix translates physically into removal and replacement of single oscillator elements. The procedure only requires the measurement of the system's spectra and subspectra to obtain the system's oscillation modes. This can be of advantage in any physical system where the modes cannot be easily measured otherwise, and simple example systems have been provided. It has been shown that the so derived modes are accurate estimates of model modes if measurements are adjusted in order to obey consistency conditions based on symmetries and the demand that eigenvalues are real. Numerical code for the reproduction of both model simulations and comparison with experimental measurements has been provided.

With only five oscillators, the considered system considered here is relatively small but allowed for resolution of all resonances in the excitation spectra. From the experimental perspective it becomes increasingly difficult to resolve all the spectral peaks as N increases. Typical linewidths of the spectrum of our experimental RF array can be assessed from our previous publication of a similar experiment [9]. From the computational perspective, larger N might cause numerical problems. For example, in order to compute the product terms in the eigenvector-eigenvalue identity it might be prudent to re-arrange the terms in Eq. (6) to avoid numerical overflow of products with many small or large factors. In addition, numerical inaccuracies in the difference terms could cause negative estimates for squared vector components. In this manuscript we have not considered the second degenerate case in the terminology of Denton et al. [2], i.e., eigenvalues of the system that occur with multiplicity larger than one. This could happen in coupled oscillator arrays for example with periodic boundary conditions. Therefore, for situations like these the provided Matlab code needs to be adjusted accordingly.

Potential applications of the successive single deletion procedure to obtain oscillation modes from measured spectra include magnetic resonance imaging (MRI). Arrays of coupled radiofrequency resonator elements are used routinely in MRI [8, 10-16]. It is well known that loading of the array with a human subject alters the eigenvalues in the dispersion relation in sometimes unpredictable ways. As a consequence, the eigenvectors, from which the RF field distribution is calculated via the Biot-Savart law, are also modified. In MRI, a single mode is typically chosen for imaging. Using the above methodology, the imaging eigenvector could be calculated in the loaded array by first measuring the full spectrum and then successively removing array elements by opening or shorting the loops remotely to obtain the subspectra. It would then be possible to iteratively adjust the capacitances C_n on the arrays to converge to the most uniform RF field distribution possible. This procedure may assist in the design of resonator arrays for example for ultra-high field MRI.

The eigenvector-eigenvalue identity can be seen as a map from the eigenvalue spectrum of a Hermitian matrix to its set of eigenvectors. The system matrix of the monomeric system considered here is in fact Hermitian and its eigenmodes could be straightforwardly estimated from measurements. The matrix of the dimeric system is non-Hermitian, but the dimeric system is in fact more interesting as it can give rise to localized edge modes [9]. We have shown that this matrix has the same eigenvalue spectrum as a similar Hermitian matrix, and a naïve application of the eigenvector-eigenvalue identity to its spectrum naturally provides the eigenvectors of the similar Hermitian matrix. The manner in which the eigenvectors of a non-Hermitian matrix can be recovered alone from its spectrum via the eigenvector-eigenvalue identity if there is a similar Hermitian matrix remains an interesting problem for the recovery of eigenmodes from systems with unknown non-Hermitian properties.

VI. DISCLOSURE

The authors and their institution, Cornell University, own patents that are related to radiofrequency resonators similar to the ones being used in this manuscript.

VII. APPENDIX

This Matlab script reproduces Fig. 1.

```
%% thompsonmodes_supplemental.m 12/20/2019
```

```
% Numerical and experimental validation of the eigenvector-eigenvalue identity
```

```
% [1] P.B. Denton, S. J. Parke, T. Tao & X. Zhang,
```

```
% "Eigenvectors from eigenvalues: a survey of a basic identity in linear algebra,"
```

```
% https://arxiv.org/abs/190803795 (2019).
```

```
% This Matlab code is part of the supplemental information of the manuscript
```

```
% [2] H.U. Voss & D.J. Ballon, "Recovery of of eigenvectors from eigenvalues
```

```
% in systems of coupled harmonic oscillators" (2019).
```

```
%%%%%%%%%%%%%%%%%%%%%%%%%%%%%%%%%%%%%%%%%%%%%%%%%%%%%%%%%%%%%%%%%%%%%%%%%
```

```
% Copyright 2019, Henning U. Voss. All rights reserved.
```

```
%
```

```
% This program is distributed in the hope that it will be useful,
```

```
% but WITHOUT ANY WARRANTY; without even the implied warranty of
```

```
% MERCHANTABILITY or FITNESS FOR A PARTICULAR PURPOSE.
```

```
%
```

```
% Redistribution and use in source and binary forms, with or without
```

```
% modification, are permitted provided that the following conditions are met:
```

```
%
```

```
% * Redistributions of source code must retain the above copyright
```

```
% notice, this list of conditions and the following disclaimer.
```

```
% * Redistributions in binary form must reproduce the above copyright
```

```
% notice, this list of conditions and the following disclaimer in
```

```
% the documentation and/or other materials provided with the distribution
```

```
%
```

```
% THIS SOFTWARE IS PROVIDED BY THE COPYRIGHT HOLDERS AND CONTRIBUTORS "AS IS"
```

```
% AND ANY EXPRESS OR IMPLIED WARRANTIES, INCLUDING, BUT NOT LIMITED TO, THE
```

```
% IMPLIED WARRANTIES OF MERCHANTABILITY AND FITNESS FOR A PARTICULAR PURPOSE
```

```
% ARE DISCLAIMED. IN NO EVENT SHALL THE COPYRIGHT OWNER OR CONTRIBUTORS BE
```

```
% LIABLE FOR ANY DIRECT, INDIRECT, INCIDENTAL, SPECIAL, EXEMPLARY, OR
```

```
% CONSEQUENTIAL DAMAGES (INCLUDING, BUT NOT LIMITED TO, PROCUREMENT OF
```

```
% SUBSTITUTE GOODS OR SERVICES; LOSS OF USE, DATA, OR PROFITS; OR BUSINESS
```

```
% INTERRUPTION) HOWEVER CAUSED AND ON ANY THEORY OF LIABILITY, WHETHER IN
```

```
% CONTRACT, STRICT LIABILITY, OR TORT (INCLUDING NEGLIGENCE OR OTHERWISE)
```

```
% ARISING IN ANY WAY OUT OF THE USE OF THIS SOFTWARE, EVEN IF ADVISED OF THE
```

```
% POSSIBILITY OF SUCH DAMAGE.
```

```
%%%%%%%%%%%%%%%%%%%%%%%%%%%%%%%%%%%%%%%%%%%%%%%%%%%%%%%%%%%%%%%%%%%%%%%%%
```

```
clear
```

```
close all
```


format short

%% Model specification

for experiment=1:2

disp(['Experiment ' num2str(experiment) ':'])

% All experimental values are in MHz and will be converted to GHz later. They have to be sorted.

switch experiment

case 1 % Monomer 200, 200, 200, 200, 200 MHz

N=5;

LC1=1./(2*pi*200e6)^2;

LC2=1./(2*pi*200e6)^2;

EV_exp=[171.3, 189.15, 205.25, 217.5, 225.2];

% The following are the original measurements before

% adjustment, so they are commented out

% EVjs_exp=[173.9, 195.45, 212.9, 224

% 176.9, 199.0, 205.1, 221.5 % The last peak was measured by placing drive into gap

% 180.8, 189.9, 215.0, 217.7

% 177.3, 197.8, 205.5, 222.3

% 173.6, 195.5, 213.2, 224.3];

% Adjust experimental subsystem eigenvalues to conform to Cauchy interlacing inequalities

% Sub-eigenvalue 3 of subsystem 2 violates Cauchy interlacing inequalities: 205.25 <= 205.1 <= 217.5

EVjs_exp=[173.9, 195.45, 212.9, 224

176.9, 199.0, 205.25, 221.5 % 3rd value adjusted

180.8, 189.9, 215.0, 217.7

177.3, 197.8, 205.5, 222.3

173.6, 195.5, 213.2, 224.3];

case 2 % Dimer with 200, 220, 200, 220, 200 MHz

N=5;

LC1=1./(2*pi*200e6)^2;

LC2=1./(2*pi*220e6)^2;

EV_exp=[178.5, 195.5, 207.0, 233.0, 239.5];

% EVjs_exp=[181.5, 201.5, 230.0, 237.5

% 183.9, 200.6, 206.8, 235.5 % The last peak was measured by placing drive into gap

% 189.0, 195.4, 227.9, 233.6

% 184.0, 199.5, 207.0, 238.4

% 181.6, 202.3, 227.5, 239.0];

% Adjust experimental subsystem eigenvalues to conform to Cauchy interlacing inequalities

% Sub-eigenvalue 3 of subsystem 2 violates Cauchy interlacing inequalities: 207 <= 206.8 <= 233

% Sub-eigenvalue 2 of subsystem 3 violates Cauchy interlacing inequalities: 195.5 <= 195.4 <= 207

EVjs_exp=[181.5, 201.5, 230.0, 237.5

183.9, 200.6, 207.0, 235.5 % 3rd value adjusted

189.0, 195.5, 227.9, 233.6 % 2nd value adjusted

184.0, 199.5, 207.0, 238.4

181.6, 202.3, 227.5, 239.0];

end

```
%% Validate the Cauchy interlacing inequalities in the measured spectrum and subspectra
```

```
for i=1:N % Subsystem index
    for j=1:N-1 % Eigenvalue index
        if not(EVjs_exp(i,j)>=EV_exp(j) && EVjs_exp(i,j)<=EV_exp(j+1))
            disp(['Sub-eigenvalue ' num2str(j) ' of subsystem ' num2str(i) ...
                ' violates Cauchy interlacing inequalities: ' ...
                num2str(EV_exp(j)) ' <= ' num2str(EVjs_exp(i,j)) ' <= ' num2str(EV_exp(j+1))])
        end
    end
end
```

```
% Conversion to GHz frequencies, to angular frequencies, and then to eigenvalues
```

```
EV_exp=(2*pi*EV_exp/1000).^(-2); EVjs_exp=(2*pi*EVjs_exp/1000).^(-2);
```

```
EVjs_exp=(EVjs_exp+EVjs_exp(end:-1:1,:))/2; % Symmetrize in row direction
```

```
%% Setting up the model system
```

```
% Details in H.U. Voss & D.J. Ballon, "Topological modes in radiofrequency resonator arrays,"
```

```
% Physics Letters A, 126177 (2020)
```

```
% Computing coupling K
```

```
K=zeros(1,4);
```

```
w1=185.5; w2=218.0; K(1)=(w2^2-w1^2)/(w1^2+w2^2);
```

```
w1=194.7; w2=204.7; K(2)=(w2^2-w1^2)/(w1^2+w2^2);
```

```
w1=197.5; w2=201.5; K(3)=(w2^2-w1^2)/(w1^2+w2^2);
```

```
w1=198.5; w2=200.5; K(4)=(w2^2-w1^2)/(w1^2+w2^2);
```

```
% Parts parameters
```

```
Ms=4.3028e-09;
```

```
L=Ms/K(1); % 26.9 microH
```

```
C1=LC1/L; % 23.6 pF
```

```
C2=LC2/L; % 19.5 pF
```

```
% Rescaling: Multiply L and C by 1e9.
```

```
% This will provide convenient but physically true GHz values for the spectrum
```

```
L=L*1e9;
```

```
C1=C1*1e9;
```

```
C2=C2*1e9;
```

```
M=L*[
```

```
    1 K(1) K(2) K(3) K(4)
```

```
    K(1) 1 K(1) K(2) K(3)
```

```
    K(2) K(1) 1 K(1) K(2)
```

```
    K(3) K(2) K(1) 1 K(1)
```

```
    K(4) K(3) K(2) K(1) 1];
```

```
%% Full system spectrum and modes
```

```
C=eye(N)*C1; for nn=2:2:N; C(nn,nn)=C2; end
```

```
H=C*M;
```

```

[EM,EV]=eig(H); % EigenModes, EigenValues
EV=diag(EV);
if iscomplex(EV); error('Model matrix H has complex eigenvalue'); end
% Sorting of eigenvalues
[EV,ind]=sort(EV,'descend'); % Descend because of the reciprocal relationship between
% eigenvalues and frequencies, the latter ones sorted in rising fashion in the experiments
EV=EV'; % All eigenvalue vectors are row vectors
EM=EM(:,ind); % The modes are column vectors here

eigenfreqs=EV.^(-.5)/(2*pi); % Relationship between eigenvalues and frequencies

%% Subspectra

% Filling up eigenvalue matrix for the N subsystems j=1..N
EVjs=zeros(N,N-1); % N row vectors of N-1 eigenvalues
for j=1:N
    Hj=H; Hj(j,:)=[]; Hj(:,j)=[]; % Remove the jth row and column
    [EMj,EVj]=eig(Hj); % Compute eigenvalues of submatrices
    EVj=diag(EVj);
    if iscomplex(EVj); error('Model submatrix has complex eigenvalue'); end
    EVj=sort(EVj,'descend');
    EVjs(j,1:N-1)=EVj';
end

% Plotting spectra
graycolor=.5*[1,1,1];
darkredcolor=.7*[1,0,0];
brightredcolor=[1,0.5,0.5];
fontsize=16;

h=figure('position',[0,150,800,800]);
subplot(1,2,1)
% Model spectra
for nn=1:N
    tmp=eigenfreqs(nn)*1000; % MHz
    plot([0,5],[tmp,tmp],'black-','linewidth',8);
    text(-.1,tmp,num2str(nn),'color','k','fontsize',fontsize);
    hold on
end
% Model subspectra
for i=1:N
    for j=1:N-1
        tmp=EVjs(i,j).^(-.5)/(2*pi)*1000; % MHz
        plot([0,5],[tmp,tmp],'-','color',graycolor,'linewidth',2);
    end
end
% Measured spectra
for nn=1:N
    tmp=EV_exp(nn).^(-.5)/(2*pi)*1000; % MHz

```

```

    plot([.5,1],[tmp,tmp],'-','color',darkredcolor,'linewidth',8);
    text(1.05,tmp,num2str(nn),'color','r','fontsize',fontSize);
end
% Measured subspectra
for i=1:N
    for j=1:N-1
        tmp=EVjs_exp(i,j).^(-.5)/(2*pi)*1000; % MHz
        plot([.5,1],[tmp,tmp],'-','color',brightredcolor,'linewidth',2);
    end
end
title('Spectra and subspectra')
xlim([-2,1.2])
set(gca,'XTick',100);
set(gca,'XTickLabel',{' '});
ymin=0.98*min(eigenfreqs*1000); ymax=1.02*max(eigenfreqs*1000);
ylim([ymin,ymax])
ylabel('Frequency\it f\rm [MHz]')
hold off

%% Thompson modes

T2=zeros(N,N); % Squared modes (mode number, mode element)
for i=1:N % Mode number
    for j=1:N % Mode vector component
        % Example N=4: counter=prod([EV(i)-EVjs(j,1),EV(i)-EVjs(j,2),EV(i)-EVjs(j,3)])
        counter=prod(EV(i)-EVjs(j,:));
        if abs(counter)<10^(-16/5*N) % For N=5, this would be 1e-16 which turned out to be a good value
            disp(['Vector component ' num2str(j) ' of model mode ' num2str(i) ...
                ' almost zero (' num2str(counter) ') and set to 0'])
            T2(i,j)=0;
        else
            subEV=EV; subEV(i)=[]; % Subspectrum
            denomin=prod(EV(i)-subEV);
            % Example N=4: denomin=prod([EV(i)-subEV(1),EV(i)-subEV(2),EV(i)-subEV(3)])
            T2(i,j)=counter/denomin;
            % The displayed indices i, j will correspond to the zeros in the EM matrix
            if T2(i,j)<0
                disp(['ERROR: Squared model vector component ' num2str(j) ...
                    ' of mode ' num2str(i) ' negative (' num2str(T2(i,j)) ')'])
            end
        end
    end
end
end
% Squared modes (mode elements, mode number) in standard notation
% in which the eigenvectors are columns of a matrix, not rows
T2=T2';
T=sqrt(T2);

% Adding a similarity transformation for non-Hermitian case.

```

```

% This has no effect on the Hermitian case
U=sqrt(C)*T;
for i=1:N; U(:,i)=U(:,i)/norm(U(:,i)); end % Normalization

% Plotting modes
subplot(1,2,2)
plotscaling=1.4;
% True model modes
for i=1:N
    plot([-0.5,N+0.5],[i,i],'k-') % Separation lines
    hold on
    tmp=abs(EM(:,i));
    tmp=tmp*plotscaling;
    plot(1:N,tmp+i,'k-', 'linewidth',8); % These to be compared with Thompson modes
    text(0.5,i+0.5,num2str(i), 'color', 'k', 'fontsize', fontsize);
end
% Non-Hermitian Thompson modes
for i=1:N
    tmp=U(:,i);
    tmp=tmp*plotscaling;
    plot(1:N,tmp+i,'k-', 'color', graycolor, 'linewidth',2);
end
title('Modes')
xlabel('Position\it n')
ylabel('Mode number\it i')
xlim([0.8,N+0.2])
ylim([1,N+1])
set(gca,'YTickLabel',{' '});

%% Experimental Thompson modes
% Comments in the model modes part

T_exp2=zeros(N,N);
for i=1:N
    for j=1:N
        counter=prod(EV_exp(i)-EVjs_exp(j,:));
        if abs(counter)<10^(-16/5*N)
            disp(['Vector component ' num2str(j) ' of experimental mode ' num2str(i) ...
                ' almost zero (' num2str(counter) ') and set to 0'])
            T_exp2(i,j)=0;
        else
            subEV_exp=EV_exp; subEV_exp(i)=[];
            denomin=prod(EV_exp(i)-subEV_exp);
            T_exp2(i,j)=counter/denomin;
        end
        if T_exp2(i,j)<0
            disp(['Squared experimental vector component ' num2str(j) ...
                ' of mode ' num2str(i) ' negative (' num2str(T_exp2(i,j)) ')'])
        end
    end
end

```

```

    end
end
T_exp2=T_exp2';
T_exp=sqrt(T_exp2);
U_exp=sqrt(C)*T_exp;
for i=1:N; U_exp(:,i)=U_exp(:,i)/norm(U_exp(:,i)); end

for i=1:N
    tmp=U_exp(:,i);
    tmp=tmp*plotscaling;
    plot(1:N,tmp+i,'r-','linewidth',2);
end
hold off
drawnow
set(h,'Color',[1 1 1])
set(h.Children,'FontName','Arial','FontSize',fontsize);
set(gcf,'InvertHardcopy','off')
set(gcf,'PaperPositionMode','auto')
saveas(h,['thompsonmodes_' num2str(experiment) '.emf'])
end

```

VIII. REFERENCES

- [1] R. C. Thompson: "Principal submatrices of normal and Hermitian matrices," *Illinois J Math*, vol. 10, pp. 296-308, 1966.
- [2] P. B. Denton, S. J. Parke, T. Tao, and X. Zhang: "Eigenvectors from eigenvalues: a survey of a basic identity in linear algebra," <https://arxiv.org/abs/190803795>, pp. 1-26, 2019.
- [3] P. B. Denton, S. J. Parke, and X. Zhang: "Eigenvalues: the Rosetta Stone for neutrino oscillations in matter," <https://arxiv.org/abs/190702534>, pp. 1-18, 2019.
- [4] P. van Mieghem: "Graph eigenvectors, fundamental weights and centrality metrics for nodes in networks," <https://arxiv.org/abs/190702534>, pp. 1-38, 2016.
- [5] D. L. Pavia, G. M. Lampman, G. S. Kriz, and J. R. Vyvyan: "Introduction to Spectroscopy" (Cengage Learning 2015, Fifth edn).
- [6] D. Ballon, M. C. Graham, S. Miodownik, and J. A. Koutcher: "A 64 MHz 1/2-birdcage resonator for clinical imaging," *J Magn Reson*, vol. 90, pp. 131-140, 1990.
- [7] M. C. Leifer: "Resonant modes of the birdcage coil," *J Magn Reson*, vol. 124, pp. 51-60, 1997.
- [8] N. De Zanche, and K. P. Pruessmann: "Algebraic method to synthesize specified modal currents in ladder resonators: Application to noncircular birdcage coils," *Magn Reson Med*, vol. 74, pp. 1470-1481, 2015.
- [9] H. U. Voss, and D. J. Ballon: "Topological modes in radiofrequency resonator arrays," *Phys Lett A*, pp. 126177, 2020.
- [10] C. E. Hayes, W. A. Edelstein, J. F. Schenck, O. M. Mueller, and M. Eash: "An efficient, highly homogeneous radiofrequency coil for whole-body NMR imaging at 1.5 T," *J Magn Reson*, vol. 63, pp. 622-628, 1985.
- [11] J. Tropp: "The theory of the bird-cage resonator," *J Magn Reson*, vol. 82, pp. 51-62, 1989.
- [12] D. Ballon, and K. L. Meyer: "Two-dimensional ladder network resonators," *J Magn Reson A*, vol. 111, pp. 23-28, 1994.
- [13] M. A. Ohliger, R. L. Greenman, R. Giaquinto, C. A. McKenzie, G. Wiggins, and D. K. Sodickson: "Concentric coil arrays for parallel MRI," *Magn Reson Med*, vol. 54, pp. 1248-1260, 2005.

- [14] H. U. Voss, and D. J. Ballon: "High-pass two-dimensional ladder network resonators for magnetic resonance imaging," *IEEE T Bio-Med Eng*, vol. 53, pp. 2590-2593, 2006.
- [15] R. Brown, Y. Wang, P. Spincemaille, and R. F. Lee: "On the noise correlation matrix for multiple radio frequency coils," *Magn Reson Med*, vol. 58, pp. 218-224, 2007.
- [16] A. Hurshkainen, A. Nikulin, E. Georget, B. Larrat, D. Berrahou, A. L. Neves, . . . R. Abdeddaim: "A novel metamaterial-inspired RF-coil for preclinical dual-nuclei MRI," *Scientific Reports*, vol. 8, pp. 9190, 2018.